American Mineralogist, Volume 72, pages 748–755, 1987

High-pressure crystal chemistry of monticellite, $CaMgSiO_4$

Z. D. Sharp
Department of Geological Sciences, University of Michigan, Ann Arbor, Michigan 48109, U.S.A.
R. M. Hazen, L. W. Finger
Geophysical Laboratory, Carnegie Institution of Washington, 2801 Upton Street, N.W., Washington, D.C. 20008, U.S.A.

Abstract

Structural refinements of a natural monticellite ($Ca_{0.99}Mg_{0.91}Fe_{0.09}Mn_{0.01}SiO_4$) were completed at seven pressures to 62 kbar using a diamond-anvil cell. Compression of monticellite is anisotropic; the orthorhombic b axis is most compressible ($\beta_b = 3.62(1) \times 10^{-4}$ kbar^{-1}), whereas the a and c axes have similar compressibilities ($\beta_a = 1.96(4) \times 10^{-4}$ kbar^{-1} and $\beta_c = 2.05(8) \times 10^{-4}$ kbar^{-1}). Monticellite axial compression ratios are 1.00:1.85:1.05, compared to ratios of 1.00:2.02:1.60 for forsterite. The bulk modulus of monticellite, assuming a Birch-Murnaghan equation of state with $K' = 4$, is 1.13(3) Mbar. The bulk moduli of the divalent cation polyhedra are 1.5(1) and 1.1(1) Mbar for the M1 (Mg) and M2 (Ca) octahedra, respectively. The Si tetrahedron, on the other hand, displays no significant compression (bulk modulus >3 Mbar) between 1 bar and 62 kbar. Monticellite compressibility and expansivity display a "noninverse" behavior, consistent with the large difference in octahedral volumes for the M1 and M2 sites.

Introduction

Crystal structures of olivine-group minerals have been studied extensively because of their importance as phases in crustal and mantle rocks, as well as because of their intrinsic crystal-chemical interest. The olivine group includes silicates of composition $^{VI}M_2^{2+}{}^{IV}SiO_4$, with Ca, Fe, Mg, and Mn as the principal M-site cations. Nonsilicate phases with the olivine structure include chrysoberyl (Al_2BeO_4), triphylite ($LiFePO_4$), and sinhalite ($MgAlBO_4$). Brown (1970, 1982) reviewed the crystal chemistry of silicate olivines at ambient conditions. There have been, in addition, numerous studies of olivine structures at high temperatures (Brown and Prewitt, 1973; Smyth and Hazen, 1973; Smyth, 1975; Hazen, 1976; Lager and Meagher, 1978; Hazen and Finger, 1987) and at high pressure (Hazen and Finger, 1980; Kudoh and Takéuchi, 1985; Kudoh and Takeda, 1986; Hazen, 1987).

In spite of this effort, there has been relatively little high-pressure research on the Ca-bearing olivines. Ca is by far the largest cation that enters the octahedral site in natural olivine (Lager and Meagher, 1978). In monticellite, Ca is strongly partitioned into the larger M2 site (Onken, 1965; Lumpkin et al., 1983), with a resulting mean M2–O bond distance of 2.37 Å, compared to a mean M1–O bond distance of 2.13 Å (Onken, 1965). In contrast, the mean M–O bond distances in both M1 and M2 sites of Fe-, Mg- and Mn-bearing olivines range from 2.10 to 2.22 Å (Brown, 1982). In many oxides and silicates, polyhedral compressibility is proportional to polyhedral volume (Hazen and Finger, 1982; Hazen, 1985). The large difference in M1 and M2 octahedral volumes in monticellite thus makes it an ideal candidate for compressibility study.

The principal objectives of this study are (1) to determine the bulk modulus and axial compressibilities of monticellite; (2) to measure the relative compressibilities of the ordered Mg, Ca, and Si cation polyhedra; (3) to relate pressure shifts in atomic positions to the anisotropic compression of monticellite; (4) to combine the high-pressure behavior with high-temperature structural variations of monticellite (Lager and Meagher, 1978) in order to derive an empirical equation of state as a function of temperature and pressure; and (5) to explain the P-T effects in terms of the monticellite crystal structure.

Experimental details

Specimen description

The monticellite specimen is from Cascade Slide, New York (Valley and Essene, 1980), and has the composition $Ca_{0.99}Mg_{0.91}Fe_{0.09}Mn_{0.01}SiO_4$ (Sharp et al., 1986) as determined by electron-microprobe analysis. A clear, inclusion-free 40 × 100 × 100 μm fragment was taken from a crushed 2-mm-diameter grain and mounted for analysis.

High-pressure crystallography

All data, both at high-pressure and at 1 bar, were collected on crystals mounted in a Merrill-Bassett–type diamond-anvil cell (Merrill and Bassett, 1974). Room-pressure data were collected under the same experimental conditions as the high-pressure data to avoid systematic errors. Data collection was made using an automated four-circle diffractometer with monochromatized Mo$K\alpha$ radiation ($\lambda = 0.70930$ Å) following the procedure of Hazen and Finger (1982). A mixture of 4:1 methanol : ethanol

0003–004X/87/0708–0748$02.00

TABLE 1. Unit-cell parameters of monticellite at various pressures

Pressure (±1 kbar)	a (Å)	b (Å)	c (Å)	V (Å)	V/V_0
0.001	4.821(2)	11.105(3)	6.381(1)	341.6(1)	1.0
11.1	4.812(3)	11.051(4)	6.364(2)	338.4(2)	0.991
20.7	4.800(2)	11.004(2)	6.346(1)	335.2(1)	0.981
29.1	4.793(2)	10.971(2)	6.335(1)	333.1(1)	0.975
41.2	4.779(2)	10.922(3)	6.317(1)	329.7(1)	0.965
53.0	4.770(2)	10.882(3)	6.305(1)	327.3(2)	0.958
61.7	4.763(1)	10.849(2)	6.294(1)	325.3(1)	0.952

Note: Values in parentheses represent estimated standard deviations (esd's).

was used as the hydrostatic pressure medium, and several 5- to 10-μm-diameter ruby chips were added for pressure calibration.

Lattice parameters at each pressure (Table 1) were refined from diffractometer angles of 15 reflections, each of which was measured in eight equivalent positions (Hamilton, 1974; King and Finger, 1979). The range of 2θ for the 15 reflections was 34–39° at all pressures in order to avoid systematic errors that result from comparing angular data from different ranges (Swanson et al., 1985). Unit-cell parameters were initially refined as triclinic; at all pressures the unit-cell angles conform to the expected orthorhombic dimensionality within two estimated standard deviations. Final values of unit-cell parameters (Table 1) were refined with orthorhombic constraints. Pressure was calibrated before and after each data collection using the ruby fluorescence method of Barnett et al. (1973). Pressure measurements have an estimated error of ±1 kbar.

Intensities were measured for all accessible reflections in a hemisphere of reciprocal space with $\sin\theta/\lambda < 0.7$ Å^{-1}. Omega step scans, with 0.025° increments and 4-s counting periods per step were used. The fixed-ϕ mode of collection was employed in order to maximize reflection accessibility and minimize attenuation of the diamond cell. A correction was made for X-ray absorption by the diamond and Be components of the diamond cell (Hazen and Finger, 1982). Digitized data for each step scan were converted to integrated intensities following the algorithm of Lehmann and Larsen (1974). Backgrounds were selected manually where necessary. Conditions of high-pressure refinements, refined atomic positional parameters, and isotropic temperature factors are given in Tables 2 and 3. Refinements were made using an ordering scheme with Ca fixed in the larger M2 site. Mg and Fe were allowed to partition equally over the M1 and remaining unfilled fraction of the M2 site (Birle et al., 1968). Calculated and observed structure factors for monticellite at seven different pressures appear in Tables 4a–4h.[1]

Data collection with reduced apertures

Low peak-to-background ratios are a significant problem in high-pressure crystallographic work. This difficulty is inherent

[1] To obtain copies of Tables 4a–4h, order Document AM-87-345 from the Business Office, Mineralogical Society of America, 1625 I Street, N.W., Suite 414, Washington, D.C. 20006, U.S.A. Please remit $5.00 in advance for the microfiche.

TABLE 2. Monticellite: Refinement conditions and refined parameters at various pressures

	1 bar	11 kbar**	11 kbar	21 kbar	29 kbar	41 kbar	53 kbar	62 kbar
No. observed ($I > 2\sigma_I$)	178	198	183	180	182	181	179	189
$R = \Sigma [F_o - F_c]/\Sigma F_o$ (%)	7.4	5.8	7.4	5.5	6.6	6.5	5.6	6.6
Weighted $R =$ $[\Sigma w(F_o - F_c)^2/\Sigma wF_o^2]^{1/2}$ (%)	4.6	3.8	4.3	3.4	4.4	4.2	4.0	4.4
Extinction† r^* ($\times 10^5$)	2.9(5)	2.4(4)	0.8(4)	1.5(4)	2.5(5)	1.9(4)	1.9(3)	1.7(3)
M1 x	0	0	0	0	0	0	0	0
y	0	0	0	0	0	0	0	0
z	0	0	0	0	0	0	0	0
B	1.04(8)	1.43(6)	1.13(8)	0.93(6)	1.03(8)	0.95(8)	1.06(7)	0.86(7)
M2 x	0.9774(7)	0.9770(4)	0.9766(6)	0.9748(4)	0.9751(7)	0.9746(6)	0.9744(5)	0.9733(6)
y	0.2771(3)	0.2764(2)	0.2763(3)	0.2766(2)	0.2765(3)	0.2761(3)	0.2754(2)	0.2757(2)
z	0.25	0.25	0.25	0.25	0.25	0.25	0.25	0.25
B	1.01(7)	1.32(5)	0.99(6)	1.00(5)	0.98(7)	1.02(6)	1.02(5)	0.94(5)
Si x	0.4111(10)	0.4122(7)	0.4099(9)	0.4116(7)	0.4117(11)	0.4102(10)	0.4117(8)	0.4134(8)
y	0.0823(4)	0.0811(3)	0.0812(3)	0.0801(3)	0.0811(4)	0.0807(4)	0.0807(3)	0.0807(3)
z	0.25	0.25	0.25	0.25	0.25	0.25	0.25	0.25
B	0.96(8)	1.25(6)	0.82(8)	0.86(6)	0.81(8)	0.93(8)	0.88(7)	0.77(7)
O1 x	0.7474(23)	0.7462(18)	0.7481(23)	0.7412(18)	0.7389(24)	0.7434(22)	0.7473(21)	0.7477(20)
y	0.0773(8)	0.0775(5)	0.0769(7)	0.0773(6)	0.0766(9)	0.0776(8)	0.0770(7)	0.0760(7)
z	0.25	0.25	0.25	0.25	0.25	0.25	0.25	0.25
B	1.17(18)	1.61(13)	1.22(17)	1.22(13)	1.57(21)	1.32(17)	1.32(15)	1.42(16)
O2 x	0.2523(23)	0.2472(17)	0.2458(23)	0.2464(18)	0.2514(24)	0.2490(21)	0.2474(21)	0.2476(20)
y	0.4494(9)	0.4478(6)	0.4484(8)	0.4477(6)	0.4483(9)	0.4471(8)	0.4456(7)	0.4461(7)
z	0.25	0.25	0.25	0.25	0.25	0.25	0.25	0.25
B	1.04(19)	1.40(13)	0.88(18)	1.15(14)	0.87(19)	0.77(16)	1.17(16)	1.11(16)
O3 x	0.2728(16)	0.2714(11)	0.2741(14)	0.2722(12)	0.2731(17)	0.2737(14)	0.2723(13)	0.2715(14)
y	0.1470(6)	0.1479(4)	0.1465(6)	0.1482(4)	0.1471(6)	0.1476(5)	0.1472(5)	0.1476(5)
z	0.0467(10)	0.0455(7)	0.0444(8)	0.0447(7)	0.0453(10)	0.0474(9)	0.0449(8)	0.0450(8)
B	1.14(13)	1.34(9)	0.84(12)	1.14(10)	1.20(14)	1.02(12)	0.92(10)	1.057(11)

Note: Values in parentheses represent esd's.
** Data in this column collected with 4-mm-diameter apertures; all other data collected with 8-mm-diameter apertures.
† Isotropic extinction coefficient as defined by Zachariasen (1967).

TABLE 3. Monticellite: Selected bond distances and angles at various pressures

Bond or angle	1 bar	11.1 kbar	20.7 kbar	29.1 kbar	41.2 kbar	53.0 kbar	61.7 kbar
M1–O1 [2]	2.210(7)	2.173(7)	2.187(6)	2.198(8)	2.172(7)	2.154(6)	2.145(6)
M1–O2 [2]	2.071(7)	2.086(7)	2.081(5)	2.060(7)	2.066(6)	2.070(6)	2.065(6)
M1–O3 [2]	2.118(7)	2.107(6)	2.109(5)	2.095(8)	2.098(6)	2.081(5)	2.078(6)
Mean M1–O [2]	2.133	2.122	2.126	2.118	2.112	2.102	2.096
O1–M1–O2 [2]	83.10(29)	82.84(26)	83.50(20)	83.45(30)	83.18(26)	83.09(23)	82.88(27)
O1–M1–O2 [2]	96.90(29)	97.16(26)	96.50(20)	96.55(30)	96.82(26)	96.91(23)	97.12(27)
O1–M1–O3 [2]	87.40(31)	87.17(31)	87.34(23)	87.78(36)	87.03(29)	87.16(27)	87.27(29)
O1–M1–O3 [3]	92.60(31)	92.83(21)	92.66(23)	92.22(36)	92.97(29)	92.84(27)	92.73(29)
O2–M1–O3 [2]	75.09(23)	74.96(28)	75.45(23)	75.50(34)	75.17(29)	75.72(26)	75.65(28)
O2–M1–O3 [2]	104.91(32)	105.04(28)	104.55(23)	104.50(34)	104.83(29)	104.28(26)	104.35(28)
M2–O1	2.502(9)	2.463(9)	2.463(7)	2.464(11)	2.434(9)	2.416(8)	2.418(8)
M2–O2	2.328(10)	2.302(10)	2.290(8)	2.303(10)	2.281(9)	2.264(9)	2.264(9)
M2–O3 [2]	2.407(7)	2.413(7)	2.394(5)	2.388(8)	2.377(6)	2.375(6)	2.369(6)
M2–O3 [2]	2.295(5)	2.278(6)	2.265(5)	2.278(7)	2.268(6)	2.257(5)	2.250(6)
Mean M2–O	2.372	2.358	2.345	2.350	2.334	2.324	2.320
O1–M2–O3 [2]	75.03(28)	74.50(28)	75.30(21)	75.69(31)	75.35(27)	75.11(24)	74.99(25)
O1–M2–O3 [2]	97.29(23)	98.30(21)	97.48(17)	97.52(25)	97.75(21)	98.16(19)	98.13(20)
O2–M2–O3 [2]	98.99(29)	99.06(29)	98.37(23)	97.89(30)	97.91(26)	97.85(25)	97.64(24)
O2–M2–O3 [2]	86.72(25)	86.05(23)	86.78(17)	86.77(27)	86.73(22)	86.59(20)	86.82(22)
O3–M2–O3 [2]	91.72(18)	91.75(16)	91.28(12)	91.70(18)	91.45(15)	91.51(13)	91.35(15)
O3–M2–O3	65.21(34)	65.69(31)	65.93(26)	65.24(36)	65.15(32)	65.99(28)	66.01(29)
O3–M2–O3	111.15(38)	110.69(34)	111.36(28)	111.25(41)	111.84(24)	110.90(30)	111.19(33)
Si–O1	1.574(12)	1.628(12)	1.582(9)	1.556(13)	1.593(11)	1.601(10)	1.593(11)
Si–O2	1.673(11)	1.647(10)	1.643(8)	1.672(12)	1.646(10)	1.654(9)	1.649(9)
Si–O3 [2]	1.626(8)	1.631(7)	1.645(6)	1.615(9)	1.612(7)	1.624(6)	1.628(7)
Mean Si–O	1.625	1.634	1.629	1.615	1.616	1.626	1.625
O1–Si–O2	116.08(54)	115.40(51)	116.35(40)	116.23(60)	116.32(50)	115.89(46)	115.89(46)
O1–Si–O3 [2]	115.17(35)	114.42(33)	114.56(25)	115.13(39)	114.48(33)	114.87(28)	115.41(27)
O2–Si–O3 [2]	101.37(41)	102.23(37)	102.49(29)	101.40(44)	102.43(37)	101.99(32)	101.66(35)
O3–Si–O3	105.82(54)	106.69(49)	104.75(39)	105.67(61)	105.10(49)	105.54(42)	104.89(45)
O1–Si	1.574(12)	1.628(12)	1.582(9)	1.556(13)	1.593(11)	1.601(11)	1.593(11)
O1–M1 [2]	2.210(7)	2.173(7)	2.187(6)	2.198(8)	2.172(7)	2.154(6)	2.145(6)
O1–M2	2.502(10)	2.463(9)	2.463(7)	2.464(11)	2.434(9)	2.416(8)	2.418(6)
Si–O1–M1 [2]	125.88(31)	124.67(31)	125.14(24)	126.05(37)	124.95(30)	124.69(28)	124.90(28)
Si–O1–M2	115.54(48)	114.84(45)	115.94(35)	115.91(53)	115.79(45)	115.22(40)	114.57(42)
M1–O1–M1	92.40(39)	94.14(41)	93.00(31)	92.18(44)	93.30(38)	94.06(36)	94.39(36)
M1–O1–M2 [2]	94.56(32)	95.79(33)	95.03(25)	94.17(38)	95.24(32)	95.55(29)	95.48(30)
O2–Si	1.673(11)	1.647(10)	1.643(8)	1.672(12)	1.646(10)	1.654(9)	1.649(9)
O2–M1 [2]	2.071(7)	2.086(7)	2.081(5)	2.060(7)	2.066(6)	2.070(6)	2.065(6)
O2–M2	2.328(10)	2.302(10)	2.290(8)	2.303(10)	2.281(9)	2.264(9)	2.264(9)
Si–O2–M1 [2]	91.83(36)	91.35(33)	91.41(26)	91.25(36)	91.16(32)	90.75(29)	91.13(31)
Si–O2–M2	117.21(61)	118.68(62)	117.82(48)	116.55(63)	117.38(55)	117.57(54)	117.05(53)
M1–O2–M1	100.78(46)	99.40(45)	99.36(36)	100.47(45)	99.72(41)	99.17(40)	99.29(40)
M1–O2–M2 [2]	123.48(27)	123.77(24)	124.08(19)	124.20(26)	124.25(23)	124.65(21)	124.57(23)
O3–Si	1.626(8)	1.631(7)	1.645(6)	1.615(9)	1.612(7)	1.624(6)	1.628(7)
O3–M1	2.118(7)	2.107(6)	2.109(5)	2.095(8)	2.098(6)	2.081(5)	2.078(6)
O3–M2	2.407(7)	2.413(7)	2.394(5)	2.388(8)	2.377(6)	2.375(6)	2.369(6)
O3–M2	2.295(7)	2.278(6)	2.265(5)	2.278(7)	2.268(6)	2.257(5)	2.250(6)
Si–O3–M1	19.49(37)	91.05(33)	90.38(24)	91.62(40)	90.97(32)	91.21(27)	91.29(30)
Si–O3–M2	94.47(29)	93.77(26)	94.60(21)	94.52(33)	94.81(27)	94.20(24)	94.52(26)
Si–O3–M2	130.10(49)	130.87(44)	130.24(36)	130.35(52)	130.75(44)	130.32(39)	129.92(40)
M1–O3–M2	99.85(30)	99.09(27)	99.20(22)	99.20(32)	98.97(27)	98.80(24)	98.81(26)
M1–O3–M2	115.72(28)	116.45(24)	115.94(21)	115.72(31)	115.33(26)	116.21(22)	116.01(24)
M2–O3–M2	118.58(30)	118.50(27)	119.32(21)	118.62(31)	118.93(26)	119.00(23)	119.25(25)

Note: Bracketed values represent bond or angle multiplicities; values in parentheses represent esd's.

in collecting data from a small crystal (i.e., with relatively small diffracting volume) mounted in a sample chamber that causes a high background of scattered radiation. It is common in high-pressure studies, therefore, for more than 50% of reflections to be unobserved, and unobserved reflections may exceed 90% in some light-atom silicates. Reducing the diameter of the diffracted-beam aperture provides one method for lowering background scatter and thus increasing the ratio of peak-to-background. A significant potential drawback of this method, however, is the possibility of cutting out a portion of the radiation diffracted from the sample.

In order to test this aperture-reduction procedure, data at 11 kbar were collected in two ways—once with fully opened 8-mm apertures and once with half-closed 4-mm apertures. By reducing the apertures the number of observed reflections increased from 183 to 198, and the weighted R decreased from 4.5 to 3.9% (Table 2). This improvement was not considered sufficient to warrant recollection of data at other pressures. In experiments with poor peak-to-background ratios, however, this procedure may result in a significant improvement in the quantity and quality of intensity data, providing that the crystal orientation is stable and well known.

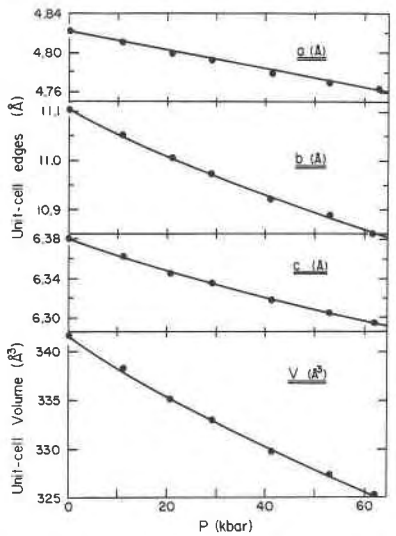

Fig. 1. Unit-cell parameters of monticellite as a function of temperature.

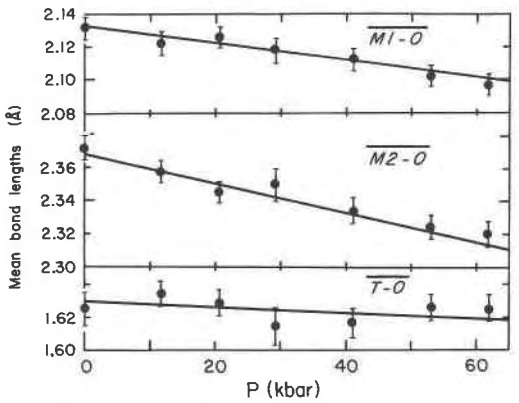

Fig. 2. Mean metal–oxygen bond distances in monticellite as a function of pressure.

Failed experiments on Ca_2SiO_4

We had hoped to combine results on monticellite with high-pressure data on the olivine form of Ca_2SiO_4. A colorless, synthetic single crystal with several 10-μm fluid inclusions was obtained from Gordon Brown, Stanford University. Unfortunately this crystal imploded at a pressure of less than 10 kbar. Such a result might have been anticipated for an inclusion-rich sample, but this is the first time that we have observed such a phenomenon. The high-pressure, single-crystal experiments on γ-Ca_2SiO_4 will be commenced as soon as we can synthesize a crystal of sufficient size.

Results

Monticellite compression and equation of state

Lattice parameters and unit-cell volumes vary smoothly as a function of pressure with no anomalous values at any pressure (Table 1, Fig. 1). Unit-cell edges as a function of pressure and average compressibilities (1 bar to 62 kbar) are as follows:

$$a = 4.8207 \pm 0.0007 - (0.00095 \pm 0.00002)P \quad (\beta_a = 1.96 \pm 0.04 \times 10^{-4}\ \text{kbar}^{-1}) \quad (1)$$

$$b = 11.104 \pm 0.002 - (0.0050 \pm 0.0002)P + (0.000015 \pm 0.000002)P^2 \quad (\beta_b = 3.62 \pm 0.01 \times 10^{-4}\ \text{kbar}^{-1}) \quad (2)$$

$$c = 6.382 \pm 0.002 - (0.0018 \pm 0.0001)P + (0.000007 \pm 0.000002)P^2 \quad (\beta_c = 2.05 \pm 0.08 \times 10^{-4}\ \text{kbar}^{-1}). \quad (3)$$

The a cell edge varies linearly with pressure, so that the second-order term is not necessary, whereas the b and c cell edges display slight curvature as a function of pressure (Fig. 1).

A least-squares fit of unit-cell volume data as a function of pressure to a Birch-Murnaghan equation of state,

$$P = 1.5K_0\{(V_0/V)^{7/3} - (V_0/V)^{5/3}\} \cdot\{1 - 0.75(4 - K')[(V_0/V)^{2/3} - 1]\}, \quad (4)$$

yields a bulk modulus $K_0 = 1.13 \pm 0.01$ Mbar if the bulk-modulus pressure derivative, K', is assumed to be 4.0 and the volume at 1 bar (V_0) = 341.6 ± 0.1 Å^3. An earlier compressibility estimate for monticellite, based on the expression $V_{\text{monticellite}} = \frac{1}{2}V_{\text{forsterite}} + \frac{1}{2}V_{\text{Ca-olivine}}$ (Sharp et al., 1986), is in excellent agreement with the measured value.

Monticellite crystal structure

The olivine-type crystal structure of monticellite (orthorhombic: *Pbnm*, Z = 4; with the mineralogical convention for olivines: $b > c > a$) was first described by Bragg and Brown (1926) and was subsequently refined by Brown (1970). The structure consists of a distorted hexagonal close-packed array of oxygens in which one-half of the octahedral sites are occupied by divalent cations and one-eighth of the tetrahedral sites contain Si.

Crystal-structure parameters of monticellite determined at 1 bar in the diamond cell are similar to previously reported values of Brown (1970) and Lager and Meagher (1978). The Mg M1 octahedron (point symmetry $\bar{1}$) has a mean Mg–O distance of 2.132 Å. It is distorted, with O–M1–O angles deviating by as much as 15° from the ideal 90° value. The Ca M2 octahedron (point symmetry m) is significantly larger than M1, with a mean Ca–O distance of 2.372 Å. The O–M2–O angles range from 65° to 111° in this highly distorted polyhedron. The Si tetrahedron (point symmetry m) has a 1.625-Å mean Si–O distance. Three O–Si–O angles are as much as 8° less than the ideal 109.5° value for a regular tetrahedron, whereas the other three angles are more than 6° greater than this value. The pairs of oxygens that define the narrower angles form shared edges between the tetrahedron and adjacent octahedra.

High-pressure crystal structures

Changes in cation–anion bond distances constitute the principal structural variations with pressure (Table 3, Fig. 2). Between 1 bar and 62 kbar the mean M1–O distance decreases from 2.132 to 2.096 Å (1.7%), whereas the mean M2–O distance compresses from 2.372 to 2.320 Å (2.2%).

TABLE 5. Monticellite: Polyhedral volume and distortion at various pressures

Atom/ parameter	1 bar	11 kbar	21 kbar	29 kbar	41 kbar	53 kbar	62 kbar
M1 (Mg)							
V (Å^3)	12.39(5)	12.20(5)	12.12(4)	12.11(6)	12.04(5)	11.91(5)	11.79(5)
QE	1.0297(14)	1.0296(13)	1.0291(11)	1.0287(15)	1.0288(13)	1.0270(12)	1.0273(12)
AV	100.6	103.8	99.48	97.6	100.2	94.6	96.0
M2 (Ca)							
V (Å^3)	16.63(7)	16.29(6)	16.09(5)	16.17(7)	15.84(6)	15.66(5)	15.59(6)
QE	1.048(4)	1.049(4)	1.046(3)	1.047(5)	1.047(4)	1.046(4)	1.046(4)
AV	164.1	167.1	158.5	159.4	163.1	158.3	158.5
Si							
V (Å^3)	2.166(17)	2.210(17)	2.187(13)	2.145(18)	2.133(16)	2.173(14)	2.164(15)
QE	1.011(5)	1.009(5)	1.010(4)	1.011(5)	1.010(5)	1.010(4)	1.011(4)
AV	50.6	39.4	43.7	49.7	43.0	45.3	50.9

Note: Values in parentheses represent esd's. QE = quadratic elongation = $\Sigma_{i=1}^{n}[(l_i/l_0)^2/(n-1)]$ (Robinson et al., 1971). AV = angle variance = $\Sigma_{i=1}^{n}[(\theta_i - \theta_0)^2/(n-1)]$ (Robinson et al., 1971).

Over this same pressure range, the mean tetrahedral Si–O distance is virtually unchanged at 1.625(10) Å. Octahedra do not compress uniformly in monticellite. In the M1 polyhedron the longest M1–O1 bonds compress 3.0%, whereas the shortest M1–O3 bonds compress only 0.2%; M1–O2 bonds of intermediate length have intermediate compression of 1.9%. The simple pattern of longer bonds being more compressible does not hold completely for the M2 octahedron. The longest M2–O1 bond is most compressible (3.5% between 1 bar and 62 kbar), but the short M2–O2 bond is next most compressible (3.0%), compared to 1.6% compression of the M2–O3 bonds with intermediate length.

There are no dramatic changes in oxygen–cation–oxygen or cation–oxygen–cation angles at high pressure. The largest systematic change occurs for the M1–O2–M2 angle, which increases from 123.5(3)° to 124.6(2)° between 1 bar and 62 kbar. The M1–O2 and M2–O2 bonds are the longest and are among the most compressible in their respective octahedra; the increase in M1–O2–M2 angle may reflect increased M1–M2 repulsion as these M–O bonds compress. No other angle changes by more than 1° over this pressure range.

Quadratic elongation (λ) and angle variance (σ^2), as defined by Robinson et al. (1971), are measures of polyhedral distortion. The quadratic elongation of the M1 and M2 polyhedra in monticellite do not vary significantly with pressure (Table 5), whereas the octahedral-angle variances decrease slightly as a function of pressure. This pressure effect is small, however, and the stronger effects of temperature (Brown and Prewitt, 1973) and composition (Robinson et al., 1971) appear to overshadow any pressure contribution to polyhedral distortion.

Polyhedral volumes for the M1, M2, and T sites (Table 5) were calculated using the program VOLCAL, written by L. W. Finger (in Hazen and Finger, 1982). Polyhedral volumes for monticellite vary linearly with pressure and are controlled predominantly by bond shortening rather than polyhedral distortion (Fig. 3). Average compressibilities (1 bar to 62 kbar) for M1 (Mg), M2 (Ca), and T (Si) are 6.8(7), 9.5(11), and 1(2) (all $\times 10^{-4}$ kbar^{-1}), respectively. The corresponding bulk moduli ($1/\beta$) are 1.5(1), 1.1(1), and >3 Mbar for the M1, M2, and T sites, respectively.

Hazen and Finger (1982) have derived an empirical equation for bulk modulus of a given polyhedron following the approach of Hazen and Prewitt (1977). This equation is

$$K_p = [7.5(2)z_c/d^3]\text{Mbar}^{-1}, \quad (5)$$

where K_p is the polyhedral bulk modulus, d is the mean cation–anion distance in ångströms, and z_c is the integral formal charge of the cation. Polyhedral moduli of monticellite predicted from Equation 5 and the mean cation–anion bond distances in Table 4 are 1.6, 1.1, and 7.0 Mbar for the M1, M2, and T sites, in good agreement with the measured values.

DISCUSSION

High-pressure vs. high-temperature structures

Monticellite volume reductions that occur upon compression are significantly different from those observed on cooling from high temperature (Lager and Meagher, 1978).[2] One of the most important differences is the relative volume change of M1 vs. M2. Thermal expansion of M1 ($\approx 1.7 \times 10^{-6}$ kbar^{-1}) is slightly greater than that of M2 ($\approx 1.3 \times 10^{-6}$ kbar^{-1}). On cooling, therefore, M1 contracts more than M2. Compression of M1, on the other hand, is less than that of M2; with increasing pressure, M2 contracts more than M1.

These differences may be quantified by considering the ratio β/α of polyhedral compressibility to thermal expansion (i.e., what temperature increase is required to offset a given pressure increase). For M1, $\beta/\alpha = [6.8 \times 10^{-4}]/[5.2 \times 10^{-5}] \approx 13$°C/kbar, close to the average value of 14°C/kbar observed by Hazen and Prewitt (1977) for Mg

[2] Note that the linear thermal expansion coefficients for monticellite and glaucochroite in Table 9 of Lager and Meagher (1978) are typeset incorrectly and should be reversed.

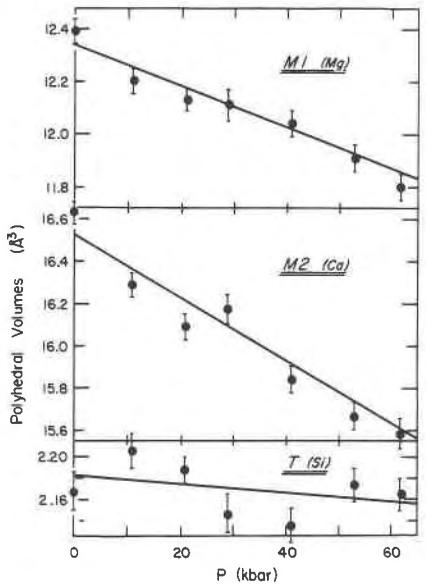

Fig. 3. Polyhedral volumes of monticellite as a function of pressure.

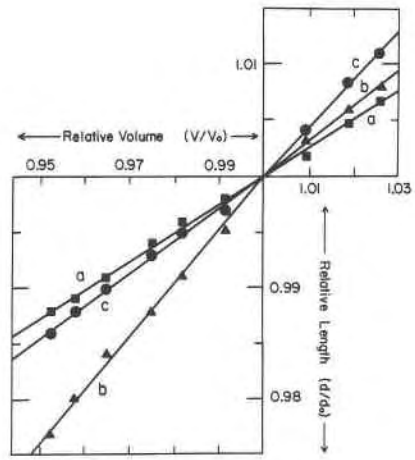

Fig. 4. Relative unit-cell parameters (d/d_0) vs. relative unit-cell volume (V/V_0) for monticellite. Circles, points, and crosses represent the *b*, *c*, and *a* axes, respectively. Points in the upper right represent high-temperature data, whereas those in the lower left represent high-pressure data.

octahedra in oxides and silicates. For M2, the value of $\beta/\alpha = [9.5 \times 10^{-4}]/[4.2 \times 10^{-5}] = 22$°C/kbar, compared to the average value of 18°C/kbar recorded by Hazen and Prewitt (1977). Note that the Si tetrahedron undergoes little, if any, volume change with either pressure or temperature increases.

The important differences in high-pressure versus high-temperature response of the M1 and M2 cation polyhedra are manifest in unit-cell behavior. The *b*-axis length, which is closely tied to M2 volume (Hazen, 1987), is almost twice as compressible as *a* or *c*. However, the *c*-axis length, which is more dependent on the size of M1, is much more expansible than *a* or *b*. A plot of relative unit-cell edge lengths versus relative unit-cell volume (Fig. 4) illustrates the significant differences between unit-cell expansion and compression. This "noninverse" behavior may be explained by considering the compressibilities and expansivities of the M1 and M2 octahedra in relation to the olivine structure.

The only unique plane of M2 octahedra in olivine is perpendicular to the *b* axis. Monticellite may, therefore, be considered as a layered structure with alternating layers of M2 octahedra and M1 and Si polyhedra perpendicular to *b*. A common feature of layered structures is that compressibility and expansivity tend to be greatest perpendicular to layering (Hazen and Finger, 1985). In monticellite, the majority of compression is expected to take place in the highly compressible M2 octahedral planes, perpendicular to the layering. Compression parallel to layering in the M2 octahedral plane will be limited by the adjacent, less compressible M1 and Si polyhedral plane.

In contrast, there is only one unique plane of M1 octahedra, and this plane is perpendicular to the *c* axis. Monticellite may be considered as alternating layers of M1 octahedra and M2-Si polyhedra perpendicular to *c*. In this case, because M1 is the most expansible polyhedron, the greatest expansion will be in the M1 octahedral plane perpendicular to *c*. Expansion parallel to layering in the M1 octahedral plane will be limited by the adjacent, more rigid M2-Si polyhedral layers. The predicted effect of pressure and temperature on monticellite, from the above crystallographic considerations, is observed in the high-pressure and high-temperature experiments.

Other olivine structures measured as a function of pressure and temperature, in contrast to monticellite, have an inverse pressure-temperature relationship. The change of lattice constants with increasing pressure can be offset by increasing temperature. However, in each of these minerals (forsterite, fayalite, and chrysoberyl), M1 and M2 have nearly identical volumes, and the compressibility and the expansivity of the M1 and M2 sites are thus nearly identical. Neither the M1 nor M2 octahedral planes will be favored during compression or expansion. For monticellite, on the other hand, there is no condition of combined high pressure and high temperature for which the lattice parameters are the same as at room conditions. This fact may, in part, explain the limited stability field of monticellite as a function of pressure and temperature.

The noninverse effect of pressure and temperature on the lattice parameters of monticellite might be used to estimate the *P-T* conditions of crystallization. Solid-inclusion piezothermometry is a method of determining *P-T* conditions during crystallization by examining a birefringent halo in a host crystal caused by the entrapment of a solid inclusion. Adams et al. (1975) determined *P-T* conditions for zero-strain birefringence in garnet that showed birefringent halos around quartz at room conditions. Piezothermometry and piezobarometry could pos-

sibly be used for monticellite. Because monticellite does not expand and compress inversely, there should be a unique pressure and temperature at which a piezometric halo around a solid inclusion would vanish. We have examined a number of grains of Cascade Slide monticellite, which crystallized at 750 ± 30°C and 7.4 ± 1 kbar (Valley and Essene, 1980). Strong birefringent halos are present around opaque inclusions in some parts of the grains. The pressure and temperature of inclusion equilibration could be determined by optical examination of these halos as a function of P and T in a heated diamond-anvil pressure cell. This technique has prospects not only for pressure and temperature estimates, but also as a measure of the degree of recrystallization during cooling in samples that do not show the piezobirefringence.

Comparison with forsterite at high pressure

The M1 sites in both forsterite and monticellite contain Mg in octahedral coordination. These M1 octahedra have nearly identical size (2.10 vs. 2.13 Å), bulk modulus (1.4 vs. 1.5 Mbar) and thermal expansion (1.6 vs. 1.7 °C^{-1}) for forsterite and monticellite, respectively (Hazen, 1976; Lager and Meagher, 1978; Kudoh and Takéuchi, 1985). The tetrahedral Si sites are also similar in these two compounds, with average Si–O distances of 1.635 Å, near-zero thermal expansion, and high bulk modulus.

The principal differences lie in the M2 sites, which contain Mg in forsterite and Ca in monticellite. The Ca-bearing polyhedron of monticellite, with mean Ca–O of 2.37 Å and volume of 16.6 Å^3, is significantly larger than the forsterite M2, with mean Mg–O of 2.13 Å and volume 13.5 Å^3. Hazen and Prewitt (1977) demonstrated that polyhedral bulk modulus is inversely proportional to polyhedral volume. The 20% larger volume of the Ca site in monticellite is thus reflected in its 20% greater bulk modulus (1.35 vs. 1.1 Mbar). Hazen and Prewitt also observed that polyhedral thermal expansion is usually dependent on Pauling bond strength (cation charge divided by coordination number) and is independent of polyhedral volume. Thus, M2 octahedra in both monticellite and forsterite are predicted to have the same thermal expansivity. Lager and Meagher (1978), however, observed monticellite M2 expansion to be 1.3×10^{-5} °C^{-1}, which is less than the 1.6×10^{-5} °C^{-1} value observed for forsterite M2 (Hazen, 1976). It is possible that the Ca-filled M2 site of monticellite is approaching a structural limit that restricts further expansion of the already large site.

Both monticellite and forsterite exhibit significant compressional anisotropy. Axial compression ratios for monticellite (a:b:c = 1.0:1.9:1.1) compare with forsterite values (1.0:2.0:1.6). The significantly greater compressibility of b compared to a is a consequence of the polyhedral linkages between rigid Si tetrahedra and more compressible octahedra (Hazen, 1987).

Stability field of monticellite

Monticellite breaks down to forsterite and merwinite by the reaction

$$\underset{\text{monticellite}}{3CaMgSiO_4} = \underset{\text{merwinite}}{Ca_3MgSi_2O_8} + \underset{\text{forsterite}}{Mg_2SiO_4}. \quad (6)$$

This reaction was reversed at 10 kbar and ~1175°C (Yoder, 1968) and has a slope of −90°C/kbar (Sharp et al., 1986). Monticellite is not stable above 25 kbar at room temperature (Yoder, 1968), and therefore, all refinements over 25 kbar were made on a metastable phase. The reduced monticellite stability range, when compared to forsterite, is thought to be related to the larger Ca cation entering the M2 site. There are, however, no obvious structural discontinuities near 25 kbar; all structural parameters vary regularly from 1 bar to 62 kbar.

The breakdown of monticellite by Reaction 6 involves the conversion of Ca in 6-fold coordination to 8-, 9- and 10-fold coordination in merwinite (Moore and Araki, 1972). The mean Ca–O bond distance for monticellite at 25 kbar is 2.35 Å. This distance represents the lower limit of mean Ca–O bonds in minerals with Ca in 6-fold coordination. If this distance is a limiting factor in controlling the stability of monticellite, then with increasing temperature, increased pressure would be necessary to compress the M2 octahedra to the point where the mean M2–O distance is 2.35 Å. However, the upper stability of monticellite has a negative slope in P-T space, in contrast to what would be expected from the above reasoning. Unlike monticellite, the forsterite-fayalite olivines have a positive P-T stability limit. The large difference in octahedral volumes for monticellite may contribute to the negative slope for the upper stability of monticellite.

The polyhedral compressibilities and expansivities in monticellite are in good agreement with those predicted from the empirical model of Hazen and Finger (1982). When consideration of polyhedral variations is combined with crystal-structure constraints, the origin of monticellite anisotropic expansion and compression, as well as the noninverse relationship between them, may be explained. It is crucial, therefore, to view expansion and compression on both the interatomic and interpolyhedral level to understand and quantify the pressure-temperature behavior of minerals.

Acknowledgments

We gratefully acknowledge constructive reviews by E. J. Essene and C. T. Prewitt. We also thank J. W. Valley and G. E. Brown for providing the specimens of monticellite and γ-Ca_2SiO_4, respectively. This research was supported in part by National Science Foundation grants EAR83-19209 and EAR84-19982.

References

Adams, H.G., Lewis, H.C., and Rosenfeld, J.L. (1975) Solid inclusion piezothermometry II: Geometric basis, calibration for the association quartz-garnet, and application to some pelitic schists. American Mineralogist, 60, 584–598.

Barnett, J.D., Block, S., and Piermarini, G.J. (1973) An optical fluorescence system for quantitative pressure measurement in the diamond anvil cell. Review of Scientific Instruments, 44, 1–9.

Birle, J.D., Gibbs, G.V., Moore, P.B., and Smith, J.V. (1968) Crystal structure of natural olivines. American Mineralogist, 53, 807–824.

Bragg, W.L., and Brown, G.B. (1926) Die Struktur des Olivins. Zeitschrift für Kristallographie, 63, 538–556.

Brown, G.E., Jr. (1970) Crystal chemistry of the olivines. Ph.D. thesis, Virginia Polytechnic Institute, Blacksburg, Virginia.

——— (1982) Olivines and silicate spinels. Mineralogical Society of America Reviews in Mineralogy, 5, 275–381.

Brown, G.E., Jr., and Prewitt, C.T. (1973) High-temperature crystal chemistry of hortonolite. American Mineralogist, 58, 577–587.

Hamilton, W.C. (1974) Angle settings for four-circle diffractometers. In International tables for X-ray crystallography, 4, 273–284. Kynoch Press, Birmingham, England.

Hazen, R.M. (1976) Effects of temperature and pressure on the crystal structure of forsterite. American Mineralogist, 61, 1280–1293.

——— (1985) Comparative crystal chemistry and the polyhedral approach. Mineralogical Society of America Reviews of Mineralogy, 14, 317–346.

——— (1987) High-pressure crystal chemistry of chrysoberyl, Al_2BeO_4: Insights on the origin of olivine elastic anisotropy. Physics and Chemistry of Minerals, 14, 13–20.

Hazen, R.M., and Finger, L.W. (1980) Crystal structure of forsterite at 40 kbar. Carnegie Institution of Washington Year Book 79, 364–367.

——— (1982) Comparative crystal chemistry. Wiley, New York.

——— (1985) Crystals at high pressure. Scientific American, 252, 110–117.

——— (1987) High-temperature crystal chemistry of phenakite (Be_2SiO_4) and chrysoberyl ($BeAl_2O_4$). Physics and Chemistry of Minerals, in press.

Hazen, R.M., and Prewitt, C.T. (1977) Effects of temperature and pressure on interatomic distances in oxygen-based minerals. American Mineralogist, 62, 309–315.

King, H.E., and Finger, L.W. (1979) Diffracted beam crystal centering and its application to high-pressure crystallography. Journal of Applied Crystallography, 12, 374–378.

Kudoh, Y., and Takeda, H. (1986) Single-crystal X-ray diffraction study on the bond compressibility of fayalite, Fe_2SiO_4, and rutile, TiO_2 under high pressure. Phisica, 139 and 140B, 333–336.

Kudoh, Y., and Takéuchi, Y. (1985) The crystal structure of forsterite Mg_2SiO_4 under high pressure up to 149 kbar. Zeitschrift für Kristallographie, 171, 291–302.

Lager, G.A., and Meagher, E.P. (1978) High-temperature structural study of six olivines. American Mineralogist, 63, 365–377.

Lehmann, M.S., and Larsen, F.K. (1974) A method for location of the peaks in step-scan–measured Bragg reflections. Acta Crystallographica, A30, 580–584.

Lumpkin, G.R., Ribbe, P.H., and Lumpkin, N.E. (1983) Composition, order-disorder and lattice parameters of olivines: Determinative methods for Mg-Mn and Mg-Ca silicate olivines. American Mineralogist, 68, 1174–1182.

Merrill, L., and Bassett, W.A. (1974) Miniature diamond anvil pressure cell for single crystal X-ray diffraction studies. Review of Scientific Instruments, 45, 290–294.

Moore, P.B., and Araki, T. (1972) Atomic arrangement of merwinite, $Ca_3Mg[SiO_4]_2$, an unusual dense-packed structure of geophysical interest. American Mineralogist, 57, 1355–1374.

Onken, H. (1965) Verfeinerung der Kristallstruktur von Monticellite. Tschermaks Mineralogische und Petrographische Mitteilungen, 10, 34–44.

Robinson, K., Gibbs, G.V., and Ribbe, P.H. (1971) Quadratic elongation: A quantitative measure of distortion in coordination polyhedra. Science, 172, 567–570.

Sharp, Z.D., Essene, E.J., Anovitz, L.M., Metz, G.W., Westrum, E.F., Jr., Hemingway, B.S., and Valley, J.W. (1986) The heat capacity of a natural monticellite and phase equilibria in the system CaO-MgO-SiO_2-CO_2. Geochimica et Cosmochimica Acta, 50, 1475–1484.

Smyth, J.R. (1975) High temperature crystal chemistry of fayalite. American Mineralogist, 60, 1092–1097.

Smyth, J.R., and Hazen, R.M. (1973) The crystal structures of forsterite and hortonolite at several temperatures up to 900°C. American Mineralogist, 58, 588–593.

Swanson, D.K., Weidner, D.J., Prewitt, C.T., and Kandelin, J.J. (1985) Single-crystal compression of γ-Mg_2SiO_4 (abs.). EOS, 66, 370.

Valley, J.W., and Essene, E.J. (1980) Akermanite in the Cascade Slide xenolith and its significance for regional metamorphism in the Adirondacks. Contributions to Mineralogy and Petrology, 74, 143–152.

Yoder, H.S., Jr. (1968) Akermanite and related melilite-bearing assemblages. Carnegie Institution of Washington Year Book 66, 471–477.

Zachariasen, W.H. (1967) A general theory of X-ray diffraction in crystals. Acta Crystallographica, 23, 558–564.

Manuscript received December 16, 1986
Manuscript accepted April 3, 1987